ELSEVIER

Thermochimica Acta 282/283 (1995) 205–224

thermochimica acta

Phase equilibria study in the partially open Cu–(O) and Me–Cu–(O) (Me = Ba, Bi, Sr) systems[1]

M. Nevřiva *, H. Kraus, D. Sedmidubský

Institute of Chemical Technology, Department of Inorganic Chemistry, Technická 5, 162 00 Praha 6, Czech Republic

Abstract

Phase equilibria in the Me–Cu–(O) systems were studied using experimental and calculation procedures. XRD and DTA were used for experimental determination of thermodynamic data. For the calculation of the phase diagrams a mathematical solution of the equations resulting from the condition of thermodynamic equilibria in partially open systems was employed. As a result the series of phase diagrams of the $SrO–CuO_x$, $BiO_{1.5}–CuO_x$ and $BaO–CuO_x$ pseudobinary systems for the various partial pressures of oxygen are presented.

Keywords: DTA; High-temperature superconductor; Me–Cu–(O) systems; Phase equilibria; Pseudobinary systems; X-ray diffraction

1. Introduction

The systems under study are the most common subsystems of the quinquenary Bi–Sr–Ca–Cu–(O) and the quaternary Y–Ba–Cu–(O) systems containing the well known high-temperature superconducting phases. Since a good knowledge of phase equilibria in these systems is of fundamental importance to their technology, the corresponding phase diagrams have been extensively studied. However, there is still a relatively wide scatter of the data reported by the various authors. This is most probably because the influence of the surrounding atmosphere on the phase equilibria was not sufficiently considered.

* Corresponding author. Tel.: + 42 2 2435 4001; fax: + 42 2 311220 6; e-mail: Milos.Nevriva@vscht.cz

[1] Dedicated to Takeo Ozawa on the Occasion of his 65th Birthday.

SSDI 0040-6031(95)02817-1

The relationship between thermodynamic behavior and partial pressure of oxygen in the atmosphere arises from the variable oxidation state of Cu which is the common component of all the studied systems. The Cu–O system has been studied since 1930 and the phase diagram has been published in Refs. [1–5]. The system includes two phases containing oxygen — cubic Cu_2O (cuprite) and monoclinic CuO (tenorite). Both phases melt congruently, the former at $T = 1229°C$ and $p_{O_2} = 32.8$ Pa, the latter at $T = 1230°C$ and $p_{O_2} = 2.49$ MPa. In the part of phase diagram between Cu_2O and CuO there is a eutectic at $T = 1090°C$, $p_{O_2} = 61.1$ kPa and composition 0.67 mol% CuO.

In the Sr–Cu–(O) system three incongruently melting phases Sr_2CuO_3 (S_2C), $SrCuO_2$ (SC), and $Sr_{14}Cu_{24}O_{41}$ ($S_{14}C_{24}$) have been detected [6–8]. Their melting temperatures decrease with increasing Cu content from $1225 \pm 5°C$ for S_2C, over $1085 \pm 5°C$ for SC down to $955 \pm 5°C$ for $S_{14}C_{24}$, the latter being very close to the eutectic temperature. Hwang et al. [6] ascribed the same temperature to both effects. The coexistence of four phases cannot, however, occur in a closed binary system at fixed pressure. Nevertheless such a situation is allowed for the system with two fixed components and varying oxygen content. It follows from our calculation that this happens at the quaternary point for the value of $P_{O_2}(=p_{O_2}/P^0)$ equal to 0.055. Moreover, we predicted by calculation and also confirmed experimentally the behavior of the $S_{14}C_{24}$ phase at P_{O_2} lower than that corresponding to this quaternary point. Under the conditions mentioned the $S_{14}C_{24}$ phase decomposes into SC and CuO below the eutectic temperature.

In the phase diagram of the Bi–Cu–(O) system there is only one intermediate Bi_2CuO_4 phase. As is apparent from literature data so far published [9–11] it has not been quite clear whether it is a congruently or incongruently melting phase.

A more complicated situation is encountered in the system Ba–Cu–(O), where a number of phases has been reported. Whereas some were confirmed to be thermodynamically stable (e.g. $BaCuO_{2+x}$ (BC), $Ba_2Cu_3O_{5+y}$ (B_2C_3), Ba_2CuO_{3+q} (B_2C) [12–16]), the stability of others (e.g. $BaCuO_{2.5}$, $BaCuO_{2.63}$ [17], $BaCu_3O_4$ [18], Ba_3CuO_4 [13], and $Ba_3Cu_5O_8$ [14]) remains unproved. Similar uncertainty is found as concerns the temperatures attributed to various invariant points observed in this system.

2. Theoretical

All the Me–Cu–(O) systems cannot be classified as closed in the thermodynamic sense because of the variable oxygen content which is evidently shared with the surrounding atmosphere, whereas the content of the other (conservative) components remains fixed. Therefore it is useful to start the thermodynamic analysis of such a system on the basis of a thermodynamic potential (hereafter called "hyperfree energy", Z) which is derived from the commonly used Gibbs free energy, G, using the Legendre transformation with respect to the chemical potential of free component [19]. For the system containing only oxygen as a free component, Z is defined by the equation

$$Z = G - \mu_O n_O \tag{1}$$

where n_O and μ_O are, respectively, the molar quantity and chemical potential of oxygen.

From the minimum of hyperfree energy representing a thermodynamic condition of equilibrium between solid (s) and liquid (l) phase in the partially open systems [19] the following equation can be derived

$$\frac{\partial Z_q(l)}{\partial Y_{c1}(l)} = \frac{Z_q(s) - Z_q(l)}{Y_{c1}(s) - Y_{c1}(l)} \tag{2}$$

where Y_{c1} means the quasimolar fraction of the fixed c1 component and Z_q is quasimolar hyperfree energy. All quasimolar quantities are defined as the original values divided by the sum of molar amounts of conservative components, e.g.

$$Z_q = \frac{Z}{\left(\sum_c n_c\right)}, \quad Y_{c1} = \frac{n_{c1}}{\left(\sum_c n_c\right)} \tag{3}$$

In this study all quantities will be presented in their quasimolar form which makes it possible to compare the various phases.

To use Eq. (2) for calculation of the phase diagram the expressions of quasimolar hyperfree energies of coexisting phases as a functions of temperature, partial pressure of oxygen, and composition are necessary. In the first step this requires construction of the model functions for Gibbs free energies on which the Legendre transformation described above is further applied.

The stable form of pure elements at 298°C and normal atmospheric pressure ($P^\circ = 101.325$ kPa) was chosen as the standard state in this work. At the standard conditions the enthalpies and entropies of the elements are defined as

$$H_q^0 = H_m^0 = 0, \quad \text{and} \quad S_q^0 = S_m^0 = \int_0^{298} C_p \, \mathrm{d} \ln (T) \tag{4}$$

respectively.

The following model functions for quasimolar hyperfree energy of individual phases have been proposed:

(1) For pure oxide MeO_γ(s) and its melt MeO_γ(l) (where Me = Ba, Bi Sr, Cu for (s) and Me = Ba, Bi, Sr for (l)) with stable oxygen content the quasimolar hyperfree energy reads

$$Z_q^{(S)}(T, P_{O_2}) = A + B \cdot T + C \cdot T \cdot \ln(T) - \frac{1}{2}\eta_O(\mu_{O_2}^0(T) + RT \ln (P_{O_2})) \tag{5}$$

and

$$Z_q^{(l)}(T, P_{O_2}) = Z_q^{(s)}(T, P_{O_2}) + \Delta H_m^M(1 - T/T^M) \tag{6}$$

respectively, where $\mu_{O_2}^0$ is the chemical potential of oxygen at $P_{O_2} = P^0$, the temperature-dependence of which is described by the relationship $\mu_{O_2}^0 = A_O +$

$B_O T + C_O T \ln(T)$, η_O is the quasimolar fraction of oxygen in a given phase ($\eta_O = 2\eta_{O_2}$), and ΔH_m^M and T^M are, respectively, the corresponding enthalpy and temperature of melting. The first three terms in Eq. (5) represent the Gibbs free energy of formation of the solid phase from the elements and the change of G associated with heating from the standard state to the temperature of interest.

(2) For construction of the hyperfree energy of the CuO_x melt with variable oxygen content the total differential described in Ref. [19] was employed. Under the condition of constant total pressure we get the relationship:

$$Z_q^{(l)}(T, P_{O_2}) = Z_q^{(l)}(T^*, P_{O_2}^*) - \int_{T^*}^{T} S_{qs}(T, \eta_O(T, P_{O_2}^*))\,dT - \frac{1}{2}R\ln(P_{O_2}^*)\int_{T^*}^{T}\eta_O(T, P_{O_2})\,dT - \frac{1}{2}RT\int_{P_{O_2}^*}^{P_{O_2}}\eta_O(T, P_{O_2})\,d\ln(P_{O_2}) \tag{7}$$

The first term $Z_q^{(l)}(T^*, P_{O_2}^*)$ is quasimolar hyperfree energy of the CuO_x melt at the starting point of integration which was chosen as the eutectic with CuO and Cu_2O reported in Ref. [1]. We can use these conditions to derive the equality

$$Z_q^{(CuO_x^l)}(T^e, P_{O_2}^e) = Z_q^{(CuO^s)}(T^e, P_O^e) = Z_q^{(Cu_2O^s)}(T^e, P_{O_2}^e) \tag{8}$$

where the values of $Z_q^{(CuO^s)}(T^e, P_{O_2}^e)$ and $Z_q^{(Cu_2O^s)}(T^e, P_{O_2}^e)$ were calculated using tabular thermodynamic data [20].

The proposed empirical relationship for the quasimolar fraction of oxygen describing its stoichiometry in the melt:

$$\eta_O(T, P_{O_2}) = 1 - (T - Q)^{1/2}(a - b(P_{O_2})^{1/3}) \tag{9}$$

is a good fit with the experimental dependence found by Roberts and Symth [1] for a broad range of partial pressure $P_{O_2}/P^0 \in \langle 10^{-3}; 10^{1} \rangle$ and temperature $T \in \langle 750; 2000 \rangle$°C. The parameters of the model Q, a, b were evaluated by the regression using the data taken from Ref. [1].

The shortened quasimolar entropy of the CuO_x melt is defined as

$$S_{qs}(T, \eta_O) = S_q(T) - \frac{1}{2}\eta_O S_{O_2}(T) \tag{10}$$

where both terms were modeled by empirical relationships. The parameters of temperature-dependence of the entropy of oxygen

$$S_{O_2}(T) = A + B\ln(T) + CT + D/T^2 \tag{11}$$

are published in thermodynamic tables [16], whereas the parameters (E, F) in the relationship for the quasimolar entropy

$$S_q(T) = E + F\ln(T) \tag{12}$$

were refined by regression of the data of Roberts and Smyth [1], verified by our experiments.

(3) For intermediate phases $Me_{1-y}Cu_yO_\delta$(s) (Me = Sr, Bi, Ba) a simple model supposing the oxygen content to be independent of both T and P_{O_2} was used. In such case the hyperfree energy

$$Z_q(T, P_{O_2}) = Y_{Cu} Z_q(CuO) + (1 - Y_{Cu}) Z_q(MeO_\gamma) + A + BT + CT\ln(T) - 1/2\Delta\eta_O RT\ln(P_{O_2}) \quad (13)$$

is constructed as a sum of hyperfree energies of the oxides forming the given phase (the first two terms), the temperature-dependence of the Gibbs energy of formation (the three terms with parameters A, B, C) and the last term reflecting the difference between the quasimolar fraction of oxygen in the intermediate phase and in the assembly of original oxides.

(4) Our thermodynamic model for the mixed oxide melt of type $Me_{1-y}Cu_yO_\delta$(l) (Me = Sr, Bi, Ba) is based on the assumption that the variable oxygen content is due only to the $CuO_x^{(l)}$ part of the melt, whereas the other part ($MeO_\gamma^{(l)}$) has a fixed oxygen content:

$$Z_q^{(l)}(T, Y_{Cu}) = Y_{Cu} Z_q(CuO_x^{(l)}) + (1 - Y_{Cu}) Z_q(MeO_\gamma^{(l)}) + RT[Y_{Cu}\ln(Y_{Cu}) + (1 - Y_{Cu}\ln(1 - Y_{Cu})] + \Omega Y_{Cu}(1 - Y_{Cu})(1 + K Y_{Cu}) \quad (14)$$

Here Ω and K are phenomenological interaction parameters of the quasiregular model used; they are dependent on P_{O_2} as follows

$$\Omega = A + B\ln(P_{O_2}) \quad (15)$$

$$K = C + D\ln(P_{O_2}) \quad (16)$$

3. Experimental

3.1. Sample preparation

Samples were prepared using BaO_2, $BaCO_3$, Bi_2O_3, CuO, and $SrCO_3$ powders as starting materials. The reagents used were chemically analyzed and the content of main components (Ba, Bi, Sr, and Cu) determined to be higher than 99.5 mol% of the theoretical amount.

Standard ceramic procedures guaranteeing the achievement of the equilibrium state consisted of one or two calcinations (for 24 h) and two or three firings steps (for 48 h) each followed by thorough homogenization. After calcination the 12 mm diameter pellets, weight approximately 2 g, were pressed from the powder before each firing. The temperatures of all preparation steps are specified in Table 1. The experiments were carried out in Pt crucibles under ambient atmosphere. During the last firing (in the case of the Ba–Cu–(O) system during all heating operations) the furnace was purged with air free from humidity and CO_2.

The phase composition of the samples was checked by X-ray diffraction analysis.

Table 1
The temperatures used for sample preparation

Calcination	Sr	Bi	Ba
	800, 850°C	700°C	800°C
Final heat treatment	900, 920, 940°C (Cu ≥ 50 qmol%) 900, 920, 965°C (Cu < 50 qmol%)	725, 750°C	870, 890, 900°C

3.2. *X-ray powder diffraction*

The X-ray diffraction analysis was performed on the DRON 3 powder diffractometer with CuK_α radiation and Ni filter. The phase composition of studied samples was checked by comparison of recorded diffractograms with those collected in the JCPDS data base.

3.3. *Differential thermal analysis*

All measurements were carried out on Netzsch apparatus, in Pt crucibles covered by lids, at the temperature ramp rate of 5 K min^{-1}. Powdered alumina was used as reference. DTA was performed in atmospheres with various P_{O_2} including purified air. Temperature data were calibrated with a set of recommended ICTA standards in the temperature range 100–1000°C. For higher temperatures (700–1450°C) the melting points of some pure metals were used. For calorimetric calibration only ICTA standards were utilized.

4. Results and discussion

4.1. *System Cu–(O)*

From the condition of equilibrium expressed as the equality of hyperfree energies a set of three equations

$$\begin{aligned} Z_q^{(CuO_x^l)}(T, P_{O_2}) &= Z_q^{(CuO^s)}(T, P_{O_2}) \\ Z_q^{(CuO_x^l)}(T, P_{O_2}) &= Z_q^{(Cu_2O^s)}(T, P_{O_2}) \\ Z_q^{(CuO^s)}(T, P_{O_2}) &= Z_q^{(Cu_2O^s)}(T, P_{O_2}) \end{aligned} \tag{17}$$

was obtained. The following parameters of the individual Z_q functions resulted from these relations upon applying the regression procedure on the experimental data of

Roberts and Smyth [1] and tabular data [20] of solid oxides and gaseous oxygen:

(1) The parameters A, B, and C in Eq. (5) for CuO and Cu_2O and for the temperature-dependence of μ_{O_2} are summarized in Table 2.

(2) The values of the parameters in the relationship for the quasimolar fraction of oxygen in CuO_x melt (Eq. (9)) are

$$a = 1.9199 \times 10^{-2}, \quad b = 4.3336 \times 10^{-3}, \quad Q = 850.68.$$

(3) The temperature-dependence of the entropy of oxygen in J mol^{-1} K^{-1} (Eq. (11)) is characterized by the parameters [20]

$$A = 15.818, \quad B = 32.556, \quad C = 2.679 \times 10^{-3}, \quad D = 2.759 \times 10^{5}.$$

(4) The parameters of the model function for the quasimolar entropy of the CuO_x melt in kJ mol^{-1} K^{-1} (Eq. (12)) were refined as

$$E = 1.7248 \times 10^{-1}, \quad F = -4.2128 \times 10^{-2}$$

(5) The starting point for the integration of the total differential (Eq. (7)) was defined by the conditions

$$T^* = 1353.15\,\text{K} \quad \text{and} \quad P^*_{O_2} = 0.5311$$

at which point the hyperfree energy of the CuO_x melt has the value $Z_q^{(CuO_x^l)}(T^*, P^*_{O_2}) = -104.461$ kJ mol^{-1}.

To verify the reliability of our model the refined parameters were substituted back into Eqs. (17) which were numerically solved. As a result the P_{O_2}–T and x–T equilibrium diagrams shown on Figs. 1(a) and 1(b), respectively, were obtained. The calculations confirmed very good agreement of the proposed model relationships with the original experimental data reported in Ref. [1], as well as with later experiments [21].

Table 2
The parameters A, B, and C of the temperature-dependence of the Gibbs free energy (in kJ mol^{-1}) for the oxides MeO_x(s) and O_2(g) [20]

Phase	A	B	C	T^M/K	H^M_m/(kJ mol^{-1})
O_2(g)	−12.388	0.03897	−0.03579	–	–
CuO	−172.707	0.31136	−0.05238	–[a]	–
Cu_2O	−267.623	0.86592	−0.13027	–[a]	–
SrO	−612.589	0.34375	−0.05842	2938	75.312
BaO	−572.817	0.32135	−0.05766	2286	58.576
α-Bi_2O_3	−612.314	0.69380	−0.12577	–[b]	–
δ-Bi_2O_3	−592.184	0.76177	−0.13849	1101	16.736

[a] The characteristics of the melting point of these oxides are dependent on P_{O_2}.
[b] Melting of this oxide does not occur under equilibrium.

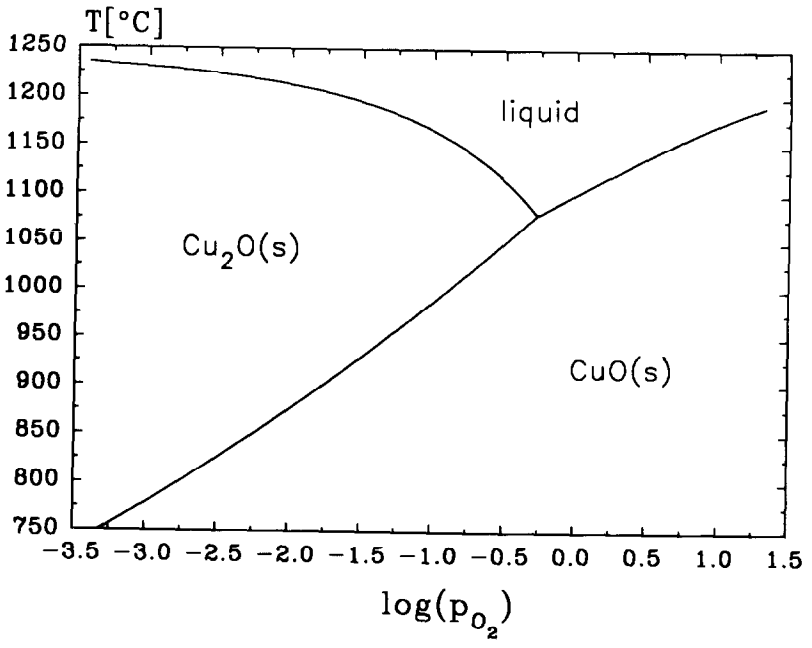

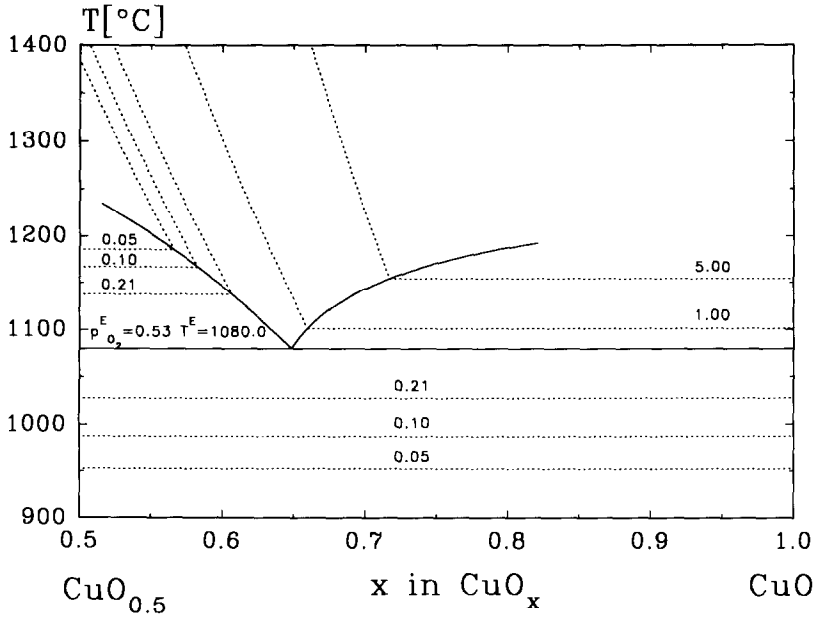

Fig. 1. Phase diagrams of Cu–(O) system calculated using the model dependence Eq. (8) for the melt CuO_x (a) P_{O_2} vs. T diagram; (b) x vs. T diagram.

4.2. System Sr–Cu–(O)

The phase equilibria in this system were examined on 23 samples of various composition in the range between S_2C and CuO_x. Their phase composition was verified by X-ray diffraction. The DTA measurements performed on these samples in pure oxygen and cleaned air ($P_{O_2} = 1$ and 0.21, respectively) provided the temperatures (± 5 K) of invariant points (one eutectic, three peritectics) and the enthalpies of melting ($\pm 10\%$). The melt composition (± 0.5 qmol%) in the invariant points was evaluated from the linear dependencies of $\Delta H = f(Y_{Cu})$ using Gäumann's method [22]. The measurements at lower values of P_{O_2} were carried out on selected specimens in two mixtures of $Ar + O_2$ and only the temperatures of invariant points were determined. All results are summarized in Table 3.

The decomposition temperature of the $Sr_{14}Cu_{24}O_{41}$ phase at lower P_{O_2} was determined by X-ray phase analysis of the samples quenched from various temperatures. The data obtained (Table 4) revealed that the temperature of decomposition decreases with decreasing P_{O_2} ($T = 822 \pm 5$°C for $P_{O_2} = 0.01$ and $T = 898 \pm 5$°C for $P_{O_2} = 0.05$). Simultaneously (Table 4) the decomposition of CuO into Cu_2O at $P_{O_2} = 0.01$ was detected at 877 ± 7°C, which is in good agreement with the value of 876°C, reported by Roberts and Smyth [1].

The respective liquidus curves were calculated by the solution of the system of Eqs. (2) after the substitution of corresponding model dependencies for hyperfree energies of coexisting phases. Invariant points (peritectics and eutectic) were found as the intersections of the calculated liquidus curves. The temperature of the solid state transition $Sr_{14}Cu_{24}O_{41} \rightarrow SrCuO_2 + CuO$ was calculated by solving the equation resulting from

Table 3
Temperatures, enthalpies, and melt compositions of eutectics and incongruent melting of the phases in the system $SrO–CuO_x$ (T – tenorite (CuO), C–cuprite (Cu_2O))

Invariant point	P_{O_2}	Y_{Cu}/qmol%	t/°C	ΔH/J g^{-1})
Peritectic S_2C	1.00	53.0	1251	226.8
Peritectic S_2C	0.21	57.5	1216	259.1
Peritectic S_2C	0.05	–	1204	–
Peritectic S_2C	0.01	–	1174	–
Peritectic SC	1.00	64.6	1112	231.9
Peritectic SC	0.21	66.8	1077	253.0
Peritectic SC	0.05	–	1049	–
Peritectic SC	0.01	–	1023	–
Peritectic $S_{14}C_{24}$	1.00	74.1	1030	357.6
Peritectic $S_{14}C_{24}$	0.21	76.0	978	375.3
Eutectic $S_{14}C_{24}$ + T	1.00	77.7	1013	725.3
Eutectic $S_{14}C_{24}$ + T	0.21	79.8	974	897.3
Eutectic SC + T	0.05	–	935	–
Eutectic SC + C	0.01	–	916	–

Table 4
Phase analysis of the quenched samples of the $Sr_{14}Cu_{24}O_{41}$ phase

$t/°C$ [a]	$P_{O_2} = 0.01$	$t/°C$ [a]	$P_{O_2} = 0.05$
	Phase composition		Phase composition
885	$SC + Cu_2O$	910	$SC + CuO$
870	$SC + CuO$	903	$SC + CuO$
830	$SC + CuO$	895	$S_{14}C_{24} + (SC + CuO)$ [b]
825	$SC + CuO + S_{14}C_{24}$ [b]	888	$S_{14}C_{24}$
820	$S_{14}C_{24} + (SC + CuO)$ [b]	880	$S_{14}C_{24}$
803	$S_{14}C_{24}$	760	$S_{14}C_{24}$

[a] Temperature from which the samples were quenched into liquid N_2.
[b] Phases present in samples only in trace amounts.

the equilibrium condition

$$Z_q^{(Sr_{14}Cu_{24}O_{41})} = xZ_q^{(SrCuO_2)} + (1-x)Z_q^{(CuO)} \tag{18}$$

where x is the phase fraction of SC in the phase group originating from the decomposition of the $S_{14}C_{24}$.

A similar approach as for Cu–(O) system was applied in order to evaluate the individual free parameters of the proposed dependencies of Z_q. The equilibrium experimental data from Tables 3 and 4, the tabular data for SrO (Table 2) and the already known parameters of the phases in the Cu–(O) system formed a consistent input set for the regression. In the model dependencies of Z_q (Eq. (13)) for $SrCuO_2$ and Sr_2CuO_3 $\Delta\eta_O$ was kept at zero, while for $Sr_{14}Cu_{24}O_{41}$ the excess of oxygen was expressed by $\Delta\eta_O = 0.079$.

The interaction parameters present in Eq. (14) for Z_q of the pseudobinary melt $Sr_{1-y}Cu_yO_x$ were found in the following form (see Eqs. (15) and (16)):

$$\Omega = -95.747 - 4.379\ln(P_{O_2}) \quad [\text{kJ mol}^{-1}]$$

$$K = -0.3262 - 0.0395\ln(P_{O_2})$$

The other refined parameters are summarized in Table 5. In contrast to the previous case (Cu–O) the Gibbs energies of formation for the solid phases were determined simultaneously with the parameters for the melt. The temperature range of the reliability of these data is therefore limited to temperatures for which the respective phases are in equilibrium with liquid phase (see Table 5). In these intervals the integral values of ΔG_f are quite reasonable, the individual parameters of their temperature-dependencies, however, do not have exact physical meaning. The same restrictions apply also to the following systems under study.

The phase diagrams calculated for $P_{O_2} = 1$, 0.21, 0.055, and 0.01 are shown in Figs. 2(a)–2(d). It is evident from comparison of the calculated liquidus curves and the transition temperatures with our experimental results (see Figs. 2(a) and 2(b)) that very

Table 5
The parameters A, B, and C of the temperature-dependence of the Gibbs free energy of formation (in kJ mol^{-1}) (Eq. (14)) for intermediate phases $Me_{1-y}Cu_yO_\delta$(s)

Phase	A	B	C	Reliability
Sr_2CuO_3	148.4	−0.872	0.105	1020–1250
$SrCuO_2$	117.1	−0.743	0.0900	820–1110
$Sr_{14}Cu_{24}O_{41}$	81.42	−0.556	0.0679	820–1030
Bi_2CuO_4	−337.9	2.340	−0.291	760–860
$BaCuO_2$	−38.94	0.213	−0.0273	900–1030
$BaCuO_2$ [a]	−399.9	2.515	−0.310	–
Ba_2CuO_3	190.7	−1.079	0.129	980–1040
Ba_2CuO_3 [a]	249.7	−1.474	0.177	–

[a] Compound prepared from $BaCO_3$.

good agreement was achieved. It is also worthy of note that although the measured liquidus temperatures were not used for the refinement, the calculated curves fit them very well. The only significant differences were observed for samples with high Cu concentration measured in air, because of the large amount of oxygen evolved during eutectic melting, which increased its local partial pressure above the melt. Thereby the liquidus temperature was systematically shifted to higher temperatures for these samples.

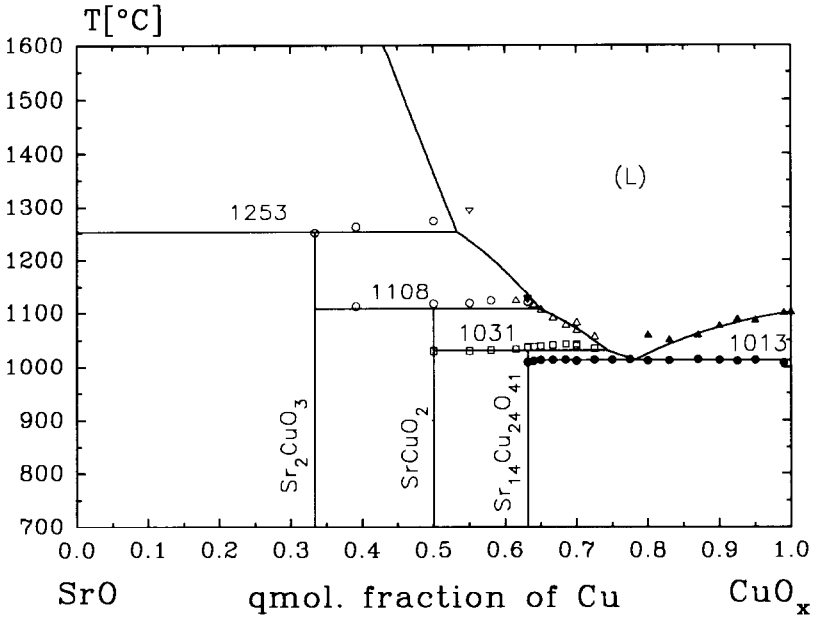

Fig. 2. Phase diagrams of Sr–Cu–(O) system calculated for various values of P_{O_2}: (a) $P_{O_2} = 1$, (b) $P_{O_2} = 0.21$ (air), (c) $P_{O_2} = 0.055$ (quaternary point), and (d) $P_{O_2} = 0.01$.

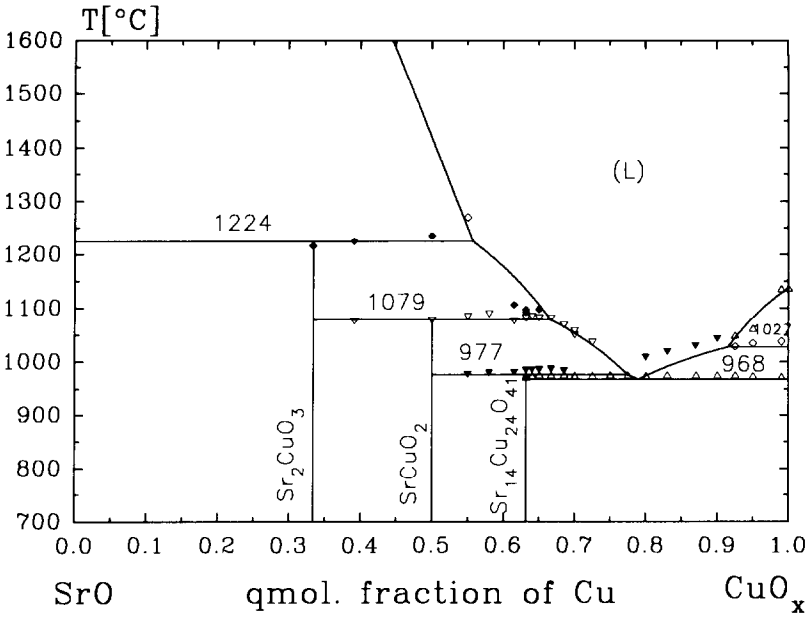
T[°C]
1600
1500
1400
1300
1200
1100
1000
900
800
700
(L)
1224
1079
977
968
1027
Sr_2CuO_3
$SrCuO_2$
$Sr_{14}Cu_{24}O_{41}$
0.0 0.1 0.2 0.3 0.4 0.5 0.6 0.7 0.8 0.9 1.0
SrO
qmol. fraction of Cu
CuO_x

Fig. 2b

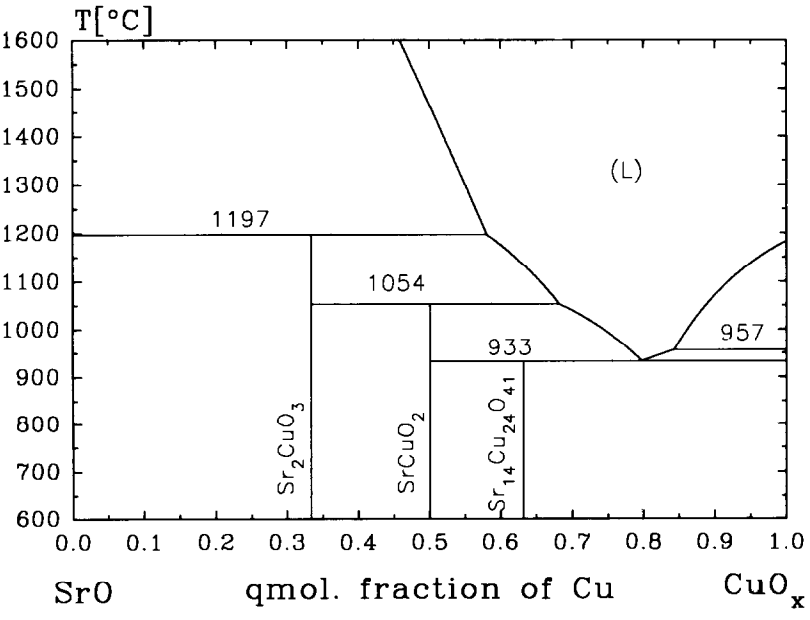
T[°C]
1600
1500
1400
1300
1200
1100
1000
900
800
700
600
(L)
1197
1054
933
957
Sr_2CuO_3
$SrCuO_2$
$Sr_{14}Cu_{24}O_{41}$
0.0 0.1 0.2 0.3 0.4 0.5 0.6 0.7 0.8 0.9 1.0
SrO
qmol. fraction of Cu
CuO_x

Fig. 2c

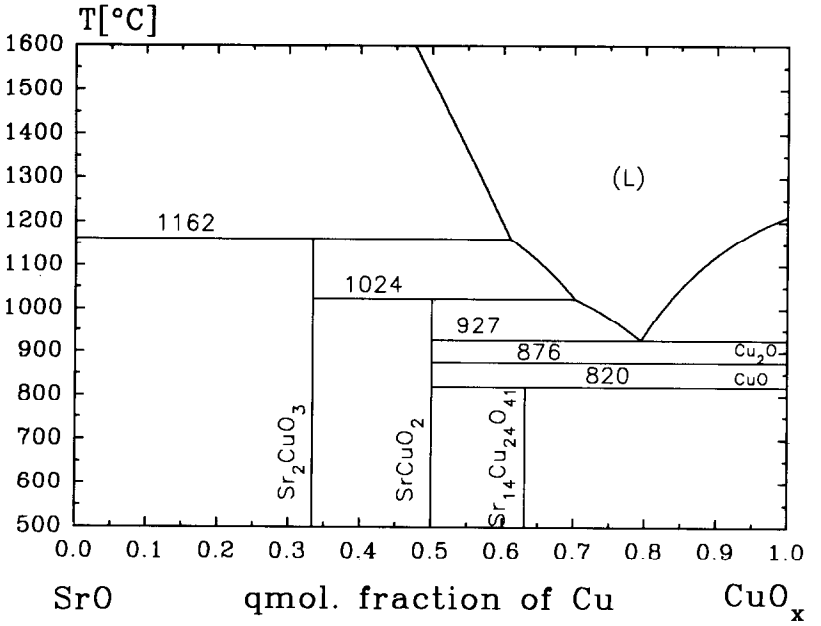

Fig. 2d

The general feature of both the calculated and the experimental results is the successive lowering of peritectic and eutectic temperatures with decreasing partial pressure of oxygen. As this decrease is more rapid for the peritectic melting of $S_{14}C_{24}$ than for the eutectic between $S_{14}C_{24}$ and CuO, both effects merge at $P_{O_2} = 0.055$ forming the first quaternary point of this system (see Fig. 2(c)). At lower P_{O_2} the phase $S_{14}C_{24}$ decomposes into CuO and SC before melting (see Fig. 2(d)). Another quaternary point is reached when the eutectic temperature and the temperature of $CuO \rightarrow Cu_2O$ decomposition become equal. This effect occurs at $P_{O_2} = 0.023$ and $T = 913°C$ when CuO, Cu_2O, $SrCuO_2$, and melt are in equilibrium. Similarly, below this P_{O_2} the CuO decomposes into Cu_2O at a lower temperature than that of melting of the eutectic $SrCuO_2 + Cu_2O$ mixture (see Fig. 2(d)).

4.3. *System Bi–Cu–(O)*

Phase equilibria in this system were determined using 17 samples from the entire composition range. The DTA measurements of all samples were carried out and evaluated in the same way as for the Sr–Cu–(O) system but in pure oxygen and cleaned air only — no experiments were performed at lower P_{O_2}. The temperatures and enthalpies of all observed effects are summarized in Table 6. The composition of the eutectics between Bi_2O_3 and Bi_2CuO_4 was found to be 7.0 qmol% Cu in oxygen and 7.2 qmol% Cu in air. The composition of peritectics was not determined.

A similar approach as for the system Sr–Cu–(O) was employed for the evaluation of the free parameters in the relevant Z_q dependencies and for the calculation of the phase

Table 6
Temperatures, enthalpies, and melt compositions of phase transitions in the Bi_2O–CuO system

Invariant point	P_{O_2}	t/°C	ΔH/(J g^{-1})
Peritectic Bi_2CuO_4	1.00	860	293.41
Peritectic Bi_2CuO_4	0.21	848	346.78
Eutectic	1.00	763	73.98
Eutectic	0.21	768	80.91
Transf. $\alpha \Rightarrow \delta$ Bi_2O_3	1.00	736	83.96
Transf. $\alpha \Rightarrow \delta$ Bi_2O_3	0.21	735	86.39
Melting δ-Bi_2O_3	1.00	828	27.02
Melting δ-Bi_2O_3	0.21	828	27.55

diagram of this system. The input set for the regression of the parameters consisted of the equilibrium experimental data from Table 6, tabular data for α- and δ-Bi_2O_3 (Table 2) and already known parameters of the phases in the Cu–(O) system.

The values found for the parameters A, B, and C of the Z_q dependence (Eq. (13)) for Bi_2CuO_4 are given in Table 5. The interaction parameters presented in the quasiregular model for the intermediate melt were found in the following form (see Eqs. (15) and (16)):

$$\Omega = -3.132 + 0.1714\ln(P_{O_2}) \quad [\text{kJ mol}^{-1}]$$

$$K = -2.518 + 0.4714\ln(P_{O_2})$$

The phase diagrams calculated for $P_{O_2} = 1$, 0.21, 0.05, and 0.01 are shown in Figs. 3(a)–3(d), respectively. Similarly to the Sr–Cu–(O) system the experimentally found liquidus temperatures are shifted to higher values for the Cu-rich samples measured in air. Our results suggest the incongruent melting of the Bi_2CuO_4 phase, as has been already reported [9, 11].

4.4. System Ba–Cu–O

Phase equilibria in this system have been extensively examined both experimentally [12–14, 21] and by calculation [23–25]. The aim of this study is to extend present knowledge by considering the influence of variable partial pressures of oxygen and to specify how the barium carbonate affects the resulting equilibria when it is used as a starting material. There are, indeed, certain indications which suggest that CO_2 or $(CO_3)^{2-}$ species can be incorporated into the crystal lattice of binary phases $BaCuO_2$ [26] and Ba_2CuO_3 [7], which could be the reason for their somewhat different thermodynamic behavior.

In order to verify and to complete our previous findings [21] we prepared four samples (with the compositions 33.3, 45, 50, and 95 qmol% Cu) from BaO_2 and three samples (50, 52, and 54 qmol% Cu) from $BaCO_3$ as starting material. These samples were investigated by DTA in oxygen and purified air. Care was explicitly taken to avoid any traces of CO_2 in the surrounding atmosphere during the preparation and DTA experiments. As a result we obtained for the former series the temperatures of

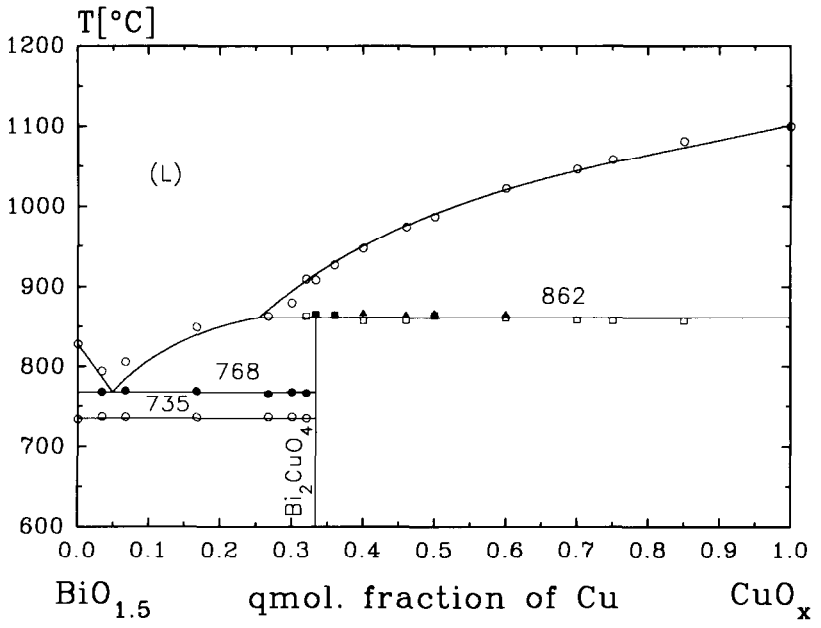

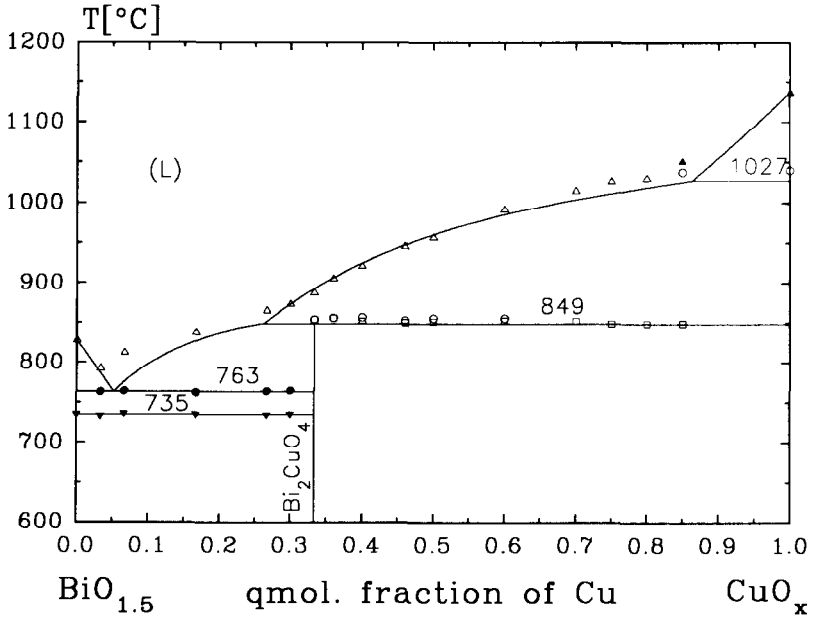

Fig. 3. Phase diagrams of Bi–Cu–(O) system calculated for various values of P_{O_2}:(a) $P_{O_2} = 1$, (b) $P_{O_2} = 0.21$ (air), (c) $P_{O_2} = 0.05$, and (d) $P_{O_2} = 0.01$.

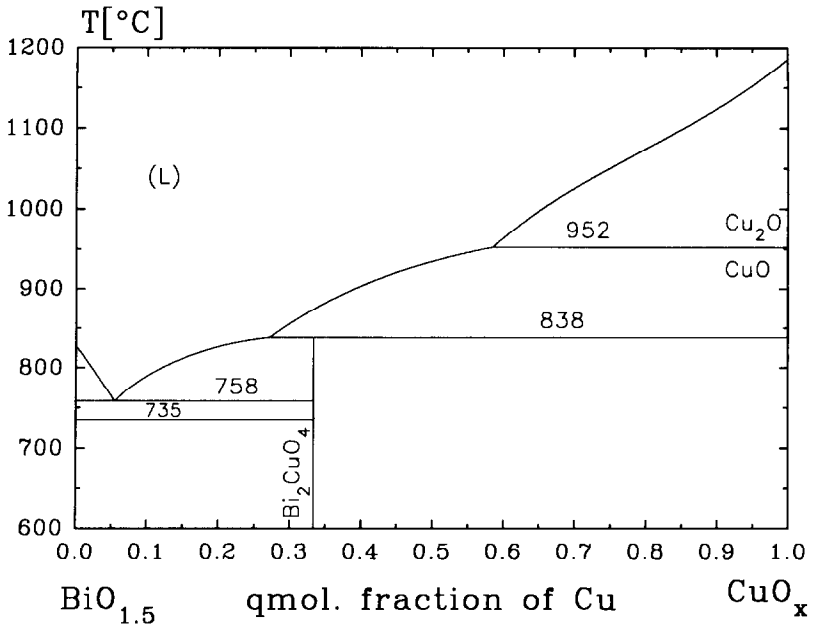
T[°C]
1200
1100
1000
900
800
700
600
(L)
952
Cu2O
CuO
838
758
735
Bi2CuO4
0.0 0.1 0.2 0.3 0.4 0.5 0.6 0.7 0.8 0.9 1.0
BiO1.5
qmol. fraction of Cu
CuOx

Fig. 3c

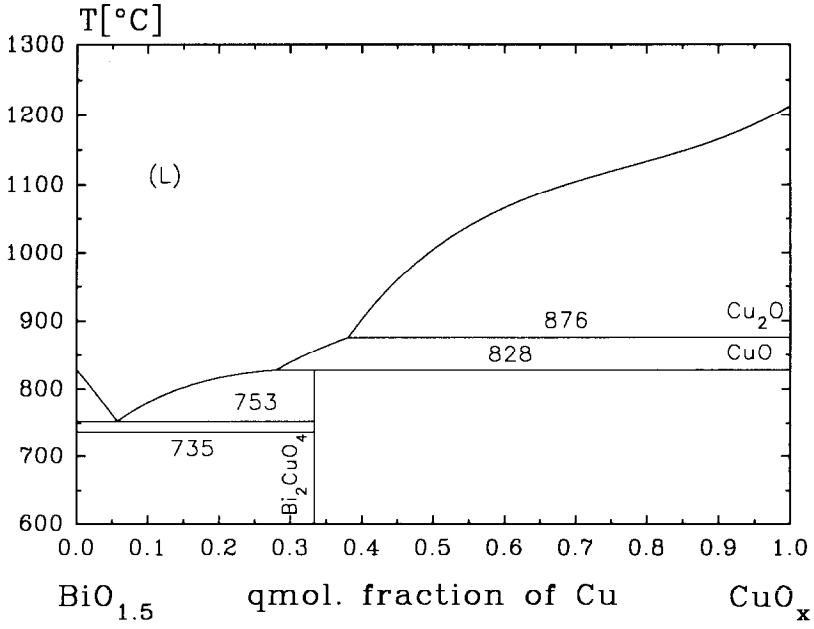
T[°C]
1300
1200
1100
1000
900
800
700
600
(L)
876
Cu2O
828
CuO
753
735
Bi2CuO4
0.0 0.1 0.2 0.3 0.4 0.5 0.6 0.7 0.8 0.9 1.0
BiO1.5
qmol. fraction of Cu
CuOx

Fig. 3d

congruent melting of $BaCuO_2$, peritectic decomposition of Ba_2CuO_3, and two eutectics, one (E_1) between $BaCuO_2$ and CuO_x, and the other (E_2) between two binary phases. The DTA records of the samples prepared from $BaCO_3$ provided the temperature of congruent melting of $BaCuO_2$ and that of Cu-rich eutectics (E_1). All experimental values are summarized in Table 7. The observed differences in both measured effects (the temperatures of congruent melting and the eutectics are higher for the samples prepared from $BaCO_3$) support our assumption that the two phases are not identical. If the latter actually contained CO_2, it would be metastable due to the inequality of chemical potentials of CO_2 in the given phase and in the atmosphere.

The two sets of data obtained on the samples prepared, respectively, from BaO_2 and $BaCO_3$, were employed, together with tabular data for solid BaO [20], the composition of eutectics between CuO and $BaCuO_2$ taken from Ref. [27], and with the previously evaluated parameters for the Cu–O system, to find the free parameters of model dependencies of the solid phases Ba_2CuO_3, $BaCuO_2$, and the binary melt $Ba_{1-x}Cu_xO_y$ (see Eqs. (13) and (14)). Both binary phases were supposed to be stoichiometric with the oxygen content independent of temperature, so that the variation of phase equilibria with P_{O_2} is only due to the behavior of the pseudobinary melt. The parameters obtained for the solid phases are included in Table 5. The refined interaction parameters of the quasibinary melt are

$$\Omega = -116.7 - 3.041\ln(P_{O_2}) \quad [\text{kJ mol}^{-1}]$$

$$K = -0.3988 - 0.0139\ln(P_{O_2})$$

for the system prepared from BaO_2, and

$$\Omega = -155.0 - 4.324\ln(P_{O_2}) \quad [\text{kJ mol}^{-1}]$$

$$K = -0.5153 - 0.022\ln(P_{O_2})$$

for the system prepared from $BaCO_3$.

The phase diagrams calculated for the "BaO_2" and "carbonate" systems, respectively, using the refined values of free parameters, are shown in Figs. 4 and 5. In each case,

Table 7
Temperatures of phase transitions in the BaO–CuO system

Invariant point	P_{O_2}	t/°C	t/°C[a]
Peritectic Ba_2CuO_3	1.00	1038	–
	0.21	1000	–
Melting $BaCuO_2$	1.00	1025	1056
	0.21	1005	1023
Eutectic 1	1.00	932	944
	0.21	905	916
Eutectic 2	1.00	999	–
	0.21	975	–

[a] $BaCO_3$ used as starting material.

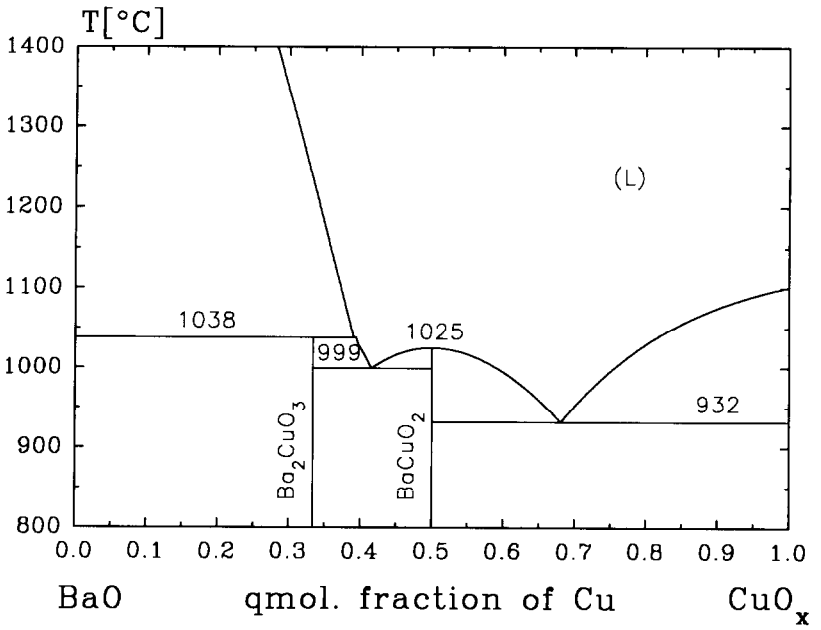

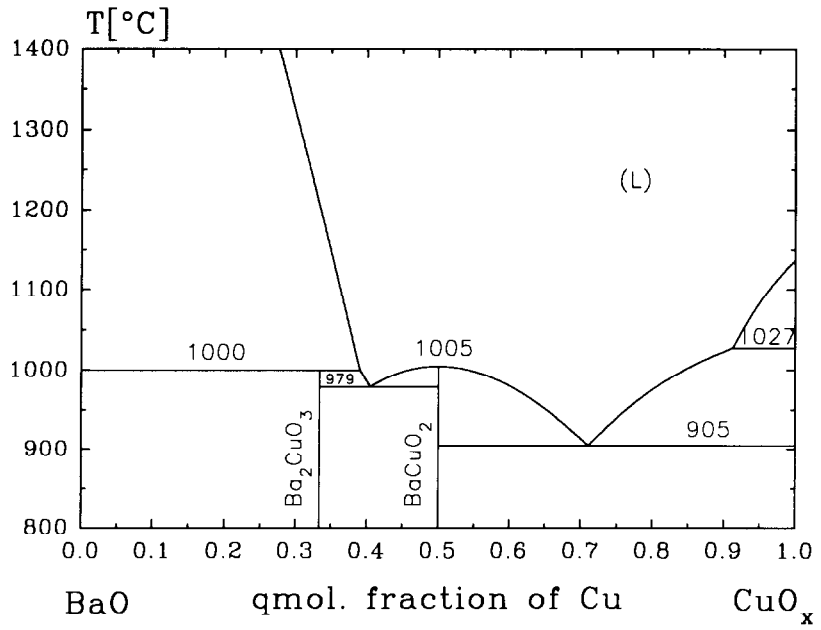

Fig. 4. Phase diagram of Ba–Cu–(O) system calculated using the parameters refined from the data measured on the samples prepared from BaO_2 as starting component. (a) $P_{O_2} = 1$ (pure oxygen), (b) $P_{O_2} = 0.21$ (air).

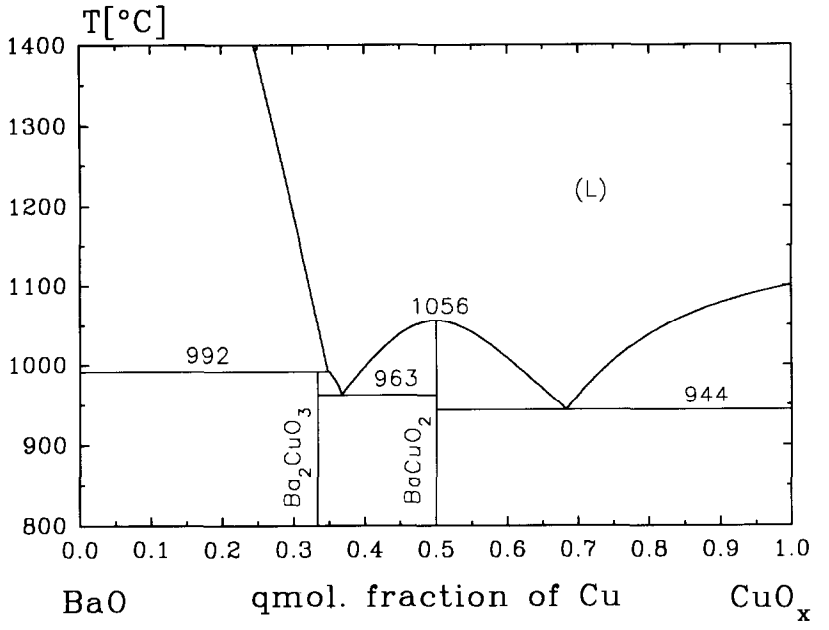

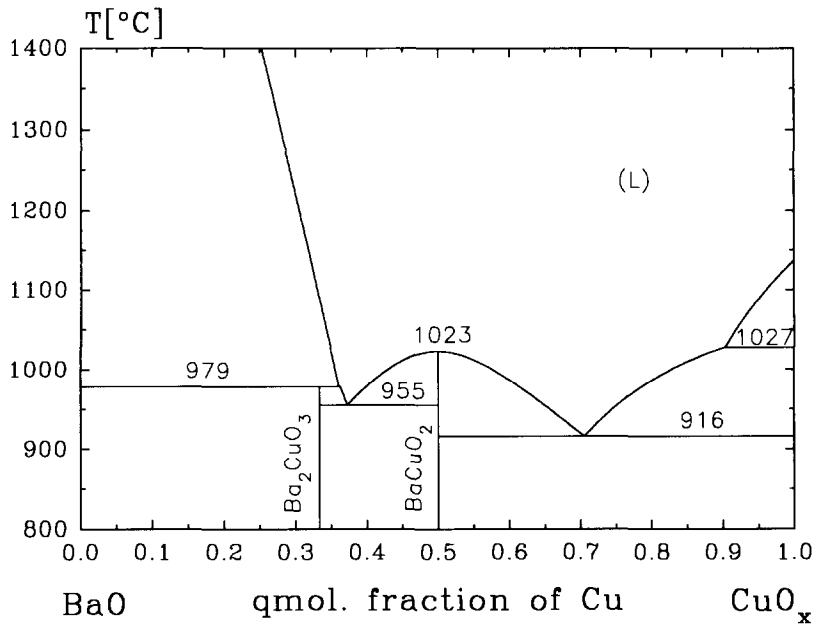

Fig. 5. Phase diagram of Ba–Cu–(O) system calculated using the parameters refined from the data measured on the samples prepared from $BaCO_3$ as starting component. (a) $P_{O_2} = 1$ (pure oxygen), (b) $P_{O_2} = 0.21$ (air).

only the results for oxygen and air atmosphere are presented. Although the experimental data were omitted from the diagrams, a quite good fit can be seen from comparison with Table 7.

5. Conclusion

A thermodynamic model has been proposed for description of the solid–liquid equilibria in Me–Cu–(O) (Me = Sr, Bi, Ba) systems. The model includes the dependence of the equilibria on oxygen partial pressure in the surrounding atmosphere, a necessary condition for appropriate thermodynamic description of such systems. Although this dependence is treated only as a result of variable oxygen content in CuO_x melt, the calculated temperatures and compositions of eutectics and peritectics correlate well with experimental observations of DTA measurements.

Acknowledgement

The research was supported by the Grant Agency of the Czech Republic (Grant No. 203/93/1167 and 104/95/0868).

References

[1] H.S. Roberts and F.H. Smyth, J. Am. Chem. Soc., 43 (1921) 1061.
[2] R. Vogel and W. Pocher, Z. Metallkd., 21 (1929) 333.
[3] J.P. Neumann, T. Zhong and Y.A. Chang, Bull. Alloy Phase Diagrams, 5(2) (1984) 136.
[4] J. Osterwald, Z. Metallkd., 21 (1968) 573.
[5] R. Schmid, Metall. Trans., 14B (1983) 473.
[6] N.M. Hwang, R.S. Roth and C.J. Rawn, J. Am. Ceram. Soc., 73 (1990) 2531.
[7] P. Karen, O. Braaten and A. Kjekshus, Acta Chem. Scand., 46 (1992) 805.
[8] K.T. Jacob and T. Mathews, J. Am. Ceram. Soc., 75 (1992) 3225.
[9] J. Cassedane, C.P. Campelo, An. Acad. Brasil. Ci., 38 (1966) 36.
[10] J.C. Boivin, D. Thomas and G. Tridot, Compt. rend. Acad. Sci., Serie C, 276 C (1973) 1105.
[11] J.F. Kargin and V.M. Skorikov, Ž. Neorg. Chim., 34 (1989) 2713.
[12] R.S. Roth, K.L. Davis and J.R. Dennis, Adv. Ceram. Mater., 2 (1987) 79.
[13] K.G. Frase, E.G. Liniger and D.R. Clarke, J. Am. Ceram. Soc., 79 (1987) C-204.
[14] D.M. De Leeuw, C.A.H.A. Mutsaers, C. Langereis, H.C.A. Smoorenburg and P.J. Rommers, Physica C, 152 (1988) 39.
[15] F. Abbatista, M. Vallino and D. Mazza, Mater. Chem. Phys., 21 (1989) 521.
[16] T. Graf, G. Triscone, A. Junod and J. Muller, J. Less-Common Met., 170 (1991) 359.
[17] M. Arjomand and D.J. Machin, J. Chem. Soc. Dalton Trans., 11 (1975) 1061.
[18] A. Bertinotti, J. Hammann, D. Luzet and E. Vincent, Physica C, 160 (1989) 227.
[19] P. Holba, Czech J. Phys., 42 (1992) 549.
[20] I. Barin and O. Knacke, Thermochemical Data of Pure Substances, Springer, Heidelberg, 1973.
[21] M. Nevřiva, E. Pollert, L. Matějková and A. Tříska, J. Crystal Growth, 91 (1988) 434.
[22] A. von Gäumann, Chimia, 20 (1966) 82.
[23] B.J. Lee and D.N. Lee, J. Am. Ceram. Soc., 72 (1989) 314.
[24] G.F. Voronin and S.A. Detgerov, J. Solid State Chem., 110 (1994) 50.
[25] I. Horsák, J. Šesták and B. Štěpánek, Thermochim. Acta, 234 (1994) 233.
[26] M.A.G. Aranda and J.P. Attfield, Angew. Chem. Int. Ed. Engl., 32 (1993) 1454.
[27] F. Licci, H.J. Scheel and P. Tissot, J. Cryst. Growth, 112 (1991) 600.